

# CONSTITUTIVE RESPONSE AND CONSISTENCY OF LEE-FENVES CONCRETE DAMAGE-PLASTICITY MODEL UNDER NON-PROPORTIONAL LOADINGS

**DIEGO FROIO<sup>\*</sup>, ROSALBA FERRARI<sup>\*</sup> AND EGIDIO RIZZI<sup>\*</sup>**

<sup>\*</sup> Università degli studi di Bergamo, Dipartimento di Ingegneria e Scienze Applicate  
viale G. Marconi 5, Dalmine (BG), I-24044, Italy  
e-mail: diego.froio@unibg.it, rosalba.ferrari@unibg.it, egidio.rizzi@unibg.it, www.unibg.it

**Key words:** Concrete Damaged Plasticity (CDP) model, Plastic strain-induced anisotropy, Constitutive driver, Non-proportional loading, Willam's test

**Abstract:** The present work attempts to address the issue of constitutive response and consistency of plastic strain-induced anisotropy of Lee-Fenves Concrete Damaged Plasticity (CDP) constitutive model. The CDP model, which comes to be available within the ABAQUS commercial FEM platform, shall be able to reproduce typical features of the failure process of quasi-brittle materials subjected to multiaxial cyclic loadings, according to FEM modelizations and simulations at the structural scale that may arise in different challenging engineering contexts. This is achieved by combining an effective stress-based nonassociative hardening/softening plasticity model, with an isotropic damage model based on plastic strains and stiffness loss/recovery capabilities during microcrack opening/closing, at a smeared continuum scale. Herein, several numerical analyses are performed, starting at a constitutive-driver level, to experiment the outcomes of the constitutive description and to quantify the amount of material anisotropy induced by plastic deformation, for representative non-proportional loading histories, which may involve the rotation of principal strains/stresses (Willam's test). Extrapolating implications and outcomes at the structural scale may then consistently follow, in the realm of significant practical applications within different structural engineering contexts.

## 1 INTRODUCTION

Nowadays, the structural analysis of large-scale concrete structures such as reactor vessels, nuclear containments, large dams and offshore platforms, for which experimental investigations are usually prohibitively expensive, still constitutes a challenging task, within the structural engineering field.

Unlike metals, concrete is a strongly heterogeneous material that exhibits several mutually interacting inelastic mechanisms such as microcrack growth, anisotropic elastic degradation, non-associated plastic flow, unstable post-failure behaviour with localization phenomena and hysteretic unloading loops, to mention only a salient few.

Therefore, the task of developing consistent and sufficiently accurate constitutive models for concrete at all stages of loading turns out to be a quite complicate challenge.

Within the framework of a typical idealization at the continuum level of the microscopic material behavior, it has widely been accepted that coupling between damage and plasticity theories shall become essential, to effectively capture the nonlinear behavior of concrete [2]. Formulations of plasticity models for concrete should also include a non-associated flow rule and an isotropic hardening rule [18].

Even though an isotropic damage description for stiffness degradation constitutes a simplified assumption, isotropic damage

models coupled with plasticity have shown to be capable of capturing concrete measured responses under nonproportional uniaxial and biaxial loading conditions ([8],[10],[11],[23]). The plastic-damage model of Lee and Fenves [10], born as an upgrade of the Barcelona model of Lubliner et al. [11], shall belong to this category. The availability of Lee and Fenves' constitutive plastic-damage model into the library of constitutive laws distributed by the ABAQUS commercial finite element software [1], with the well-known acronym of Concrete Damaged Plasticity (CDP) model, has boosted its widespread application in both academic research and engineering practice, for the nonlinear analysis of concrete structures.

The CDP model describes in an efficient fashion several of the basic features of the mechanical nonlinear behaviour of concrete: isotropic strength and stiffness degradation (strain-softening) under tension, compression and tension-compression stress (or strain) states, strength and ductility increase in compression under increasing lateral confinement, development of permanent (plastic) strains and Microcracks Closing-Reopening (MCR) effects. However, no damage-induced anisotropy can occur at the material point level, as herein shown, whereas plastic strain-induced anisotropy shall theoretically take place. Therefore, an attempt of evaluating the extent of such anisotropy driven only by plastic strains seems pertinent, in order to draw some conclusions about its influence on the CDP material response. This issue is tackled in the present paper, where various numerical experiments are performed at a constitutive-driver level, to evaluate the amount of rotation of principal stress directions under prescribed rotating principal directions of strains, as dictated by Willam's test [21].

The present paper is organized as follows. The constitutive formulation of the CDP model is briefly summarized, in its main relations, in Section 2, where the conditions under which an anisotropic behaviour may be predicted by the CDP model under multiaxial stress states are also explored. The extent of plastic strain-induced anisotropy predicted by the CDP model for increasing values of CDP dilatancy factor

and cumulated plastic strains is discussed in detail in Section 3, where the outcomes of numerical analyses performed at a constitutive-driver level within the ABAQUS platform are presented for representative biaxial non-proportional loading histories (Willam's test). Closing considerations are finally outlined in Section 4.

## 2 CONCRETE DAMAGED PLASTICITY (CDP) MODEL

### 2.1 General constitutive relations

In this section, the fundamental relations of the rate-independent CDP model are illustrated within the corresponding small strains framework. Index tensor notation is adopted (the repetition of Latin indices implying summation from 1 to 3, according to Einstein summation convention). An overdot denotes material time derivative, i.e. the rate of a given quantity; since the considered constitutive model is rate-independent, the rates must be interpreted as linked to infinitesimal increments of the loading history described by parameter  $\tau$ . A state index  $\iota \in \{t, c\}$  is here adopted, where  $t$  denotes tensile-dominated stress states and  $c$  compression-dominated stress states.

The general incremental relations of the CDP model are here briefly summarized:

$$\dot{\varepsilon}_{ij} = \dot{\varepsilon}_{ij}^e + \dot{\varepsilon}_{ij}^p; \quad (1a)$$

$$\dot{\sigma}_{ij} = (1 - D)\dot{\bar{\sigma}}_{ij} - \dot{D}\bar{\sigma}_{ij}, \quad \dot{\bar{\sigma}}_{ij} = E_{ijkl}^0 \dot{\varepsilon}_{kl}; \quad (1b)$$

$$1 - D = [1 - r(\bar{\sigma}_{ij})D_t(\kappa_t)](1 - D_c(\kappa_c)); \quad (1c)$$

$$\dot{\varepsilon}_{ij}^p = \lambda \frac{\partial g(\bar{\sigma}_{ij})}{\partial \bar{\sigma}_{ij}}; \quad (1d)$$

$$\kappa_t = \frac{1}{g_t^{pf}} \int_0^{\varepsilon_{t,M}^p} f_t(\kappa_t) r(\bar{\sigma}_{ij}) d\varepsilon_t^p;$$

$$\kappa_c = \frac{1}{g_c^{pf}} \int_0^{\varepsilon_{III,m}^p} f_c(\kappa_c) [1 - r(\bar{\sigma}_{ij})] d\varepsilon_{III}^p; \quad (1e)$$

$$\varepsilon_{I,M}^p = \max\{\varepsilon_I^p\}, \quad \varepsilon_{III,m}^p = \min\{\varepsilon_{III}^p\};$$

$$\lambda \geq 0, \quad \dot{f}(\bar{\sigma}_{ij}, \kappa_\iota) \leq 0, \quad \lambda \dot{f}(\bar{\sigma}_{ij}, \kappa_\iota) = 0. \quad (1f)$$

Eq. (1a) represents the usual additive decomposition of small strain rate tensor  $\dot{\varepsilon}_{ij}$  into an elastic part ( $\dot{\varepsilon}_{ij}^e$ ) and a plastic part ( $\dot{\varepsilon}_{ij}^p$ ).

Eq. (1b) constitutes the incremental form of the elastic stress-strain relation, where  $\sigma_{ij}$  and  $\bar{\sigma}_{ij}$  are the nominal and effective stress tensors, respectively, which are related according to the principle of strain equivalence as

$$\sigma_{ij} = (1 - D)\bar{\sigma}_{ij}; \quad (2)$$

through scalar damage variable  $0 \leq D \leq 1$ , introduced to represent the isotropic degradation of the secant elastic stiffness, whereas

$$E_{ijkl}^0 = \lambda_0 \delta_{ij} \delta_{kl} + 2G_0 \frac{1}{2} (\delta_{ik} \delta_{jl} + \delta_{il} \delta_{jk}); \quad (3)$$

$$\lambda_0 = \frac{\nu_0 E_0}{(1 + \nu_0)(1 - 2\nu_0)}, \quad G_0 = \frac{E_0}{2(1 + \nu_0)};$$

is the fourth-order isotropic elastic stiffness tensor of the intact (undamaged) material, depending on Lamé's constants  $\lambda_0, G_0$  ( $E_0$ : Young's modulus,  $\nu_0$ : Poisson's ratio), and  $\delta_{ij}$  is Kronecker's delta.

Eq. (1c) characterizes the approach proposed by Lee and Fenves (1998) [10] to reproduce MCR effects, by means of two inherent stiffness degradation variables, to account for different damage states mainly occurred during tensile stress states ( $D_t$ ) and compressive stress states ( $D_c$ ), and an isotropic weight function  $0 \leq r \leq 1$  of the effective stress inducing a stiffness recovery effect:

$$r(\bar{\sigma}_{ij}) = \begin{cases} 0 & \text{if } \bar{\sigma}_{ij} = 0 \\ \frac{\sum_{K=1}^3 \langle \bar{\sigma}_K \rangle}{\sum_{K=1}^3 |\bar{\sigma}_K|} & \text{otherwise;} \end{cases} \quad (4)$$

where  $\langle \cdot \rangle$  is the McAulay bracket operator (so-called positive part or ramp function) and  $\bar{\sigma}_K$  ( $K = 1, 2, 3$ ) are the principal values of the effective stress tensor.

Eq. (1d) represents the non-associative flow rule expressing  $\dot{\varepsilon}_{ij}^p$  as the gradient of a scalar function  $g(\bar{\sigma}_{ij})$  of the effective stress, so-called plastic potential, scaled by non-negative plastic consistency multiplier  $\dot{\lambda}$ . Since the Drucker-Prager (DP) function of the original Lee and Fenves' CDP model displays a singular point at the origin (apex of the cone), which should be avoided for numerical reasons, the following

DP hyperbolic function has been implemented into the ABAQUS platform [1]:

$$g(\bar{\sigma}_{ij}) = \sqrt{(\alpha'_d f_{ct0} e)^2 + 3\bar{J}_2} - \frac{1}{3} \alpha'_d \bar{I}_1; \quad (5)$$

where  $\bar{I}_1 = \text{tr}(\bar{\sigma}_{ij}) = \bar{\sigma}_{ii}$  is the first invariant of the effective stress tensor,  $\bar{J}_2 = \bar{s}_{ij} \bar{s}_{ij} / 2$  is the second invariant of the effective stress deviatoric tensor  $\bar{s}_{ij} = \bar{\sigma}_{ij} - \bar{I}_1 / 3 \delta_{ij}$ ,  $f_{ct0}$  is the uniaxial tensile stress at failure of the undamaged material,  $\alpha'_d$  is the dilatancy factor associated with the definition of  $g$  as expressed by Eq. (5), while parameter  $e$ , referred to as eccentricity, controls the rate at which the function approaches its asymptotic trend ( $g$  tends to a straight line in the  $\bar{p}$ - $\bar{q}$  plane, as  $e \rightarrow 0$ , where  $\bar{p} = \bar{I}_1 / 3$  and  $\bar{q} = \sqrt{3\bar{J}_2}$ ).

Eqs. (1e) express the two hardening/softening rules for the evolution of two independent internal variables  $0 \leq \kappa_t \leq 1$  ( $t \in \{t, c\}$ ), which resemble the hardening variables of classical plasticity in that they never decrease, and they increase if and only if plastic deformations take place. These variables determine the evolution of both tensile/compressive strengths  $f_t(\kappa_t), f_c(\kappa_c)$  and different damage states  $D_t(\kappa_t), D_c(\kappa_c)$  arising under tensile and compressive loading. Four functions  $f_t, f_c, D_t, D_c$ , either expressed in terms of  $\kappa_t, \kappa_c$  or directly in terms of maximum and minimum plastic strains  $\varepsilon_t^p, \varepsilon_{III}^p$  must be supplied, as input material data to the CDP model.

Quantities  $g_t^{pf}$  and  $g_c^{pf}$  are the dissipated energy densities by plastic deformations, i.e. the areas underneath the complete stress-plastic strain curves, in uniaxial tension and in uniaxial compression, respectively. The corresponding overall dissipated energy densities during the entire process of microcracking (plasticity plus stiffness degradation) are herein denoted by  $g_t^f$  and  $g_c^f$ ; such dissipated energy densities are known to depend on the size of the localization zone, to maintain the objectivity of the constitutive evolution within the softening regime. Because the capacity for the dissipated energy per unit volume cannot be given as a material property,  $g_t^f$  ( $t = t, c$ ) should be derived from other known material properties

such as the fracture energy. Assuming that the fracture energy in the uniaxial tensile state ( $G_t^f$ ) and its counterpart in the uniaxial compressive state ( $G_c^f$ ) are given as material properties, each  $g_t^f$  is equal to the corresponding fracture energy normalized by the localization zone size  $l_t^{ch}$ , also referred to as the material characteristic length or crack band width (Bažant and Oh, 1983 [3]), which leads to  $g_t^f = G_t^f / l_t^{ch}$ . In FEM analysis, the material characteristic lengths may be substituted by element characteristic length  $l^e$ , toward a fracture-energy based regularization. For the present study, carried out at the material point level, the value of  $l^e$  is immaterial and, thus, is set equal to unity.

Eqs. (1f) are the Kuhn-Tucker (KT) conditions expressing the loading/unloading criterion at the yield limit ( $f = 0$ ). Isotropic yield/failure function  $f$ , which limits the current admissible stress states ( $f \leq 0, \dot{\lambda}f = 0$ ) and evolves with the loading process, assumes the following form:

$$f(\bar{\sigma}_{ij}, \kappa_t) = \frac{\sqrt{3}\bar{J}_2 + \alpha\bar{I}_1 + \beta(\kappa_t)\bar{\sigma}_I}{1 - \alpha} - \bar{f}_c(\kappa_c); \quad (6)$$

where dimensionless coefficient

$$\beta(\kappa_t) = \begin{cases} (1 - \alpha) \frac{\bar{f}_c(\kappa_c)}{\bar{f}_t(\kappa_t)} - (1 + \alpha) & \bar{\sigma}_I \geq 0; \\ \gamma & \bar{\sigma}_I \leq 0 \end{cases}; \quad (7)$$

varies through the loading history,  $\bar{f}_t = f_t / (1 - D_t)$  and  $\bar{f}_c = f_c / (1 - D_c)$  are the tensile and compressive strengths of the intact material, respectively, whereas  $\alpha, \gamma$  are two characteristic parameters affecting the shape of  $f$ .

Hence, the plastic part of Lee-Fenves' CDP model is based on the effective stress and is defined by the yield function, the non-associated flow rule, the evolution law for the hardening variables and the loading-unloading conditions. Damage is directly predicted by cumulated plastic deformations through imposed functions  $D_t(\kappa_t)$  and  $D_c(\kappa_c)$ . This implies that stiffness degradation cannot occur independently from plastic deformation (single-dissipative material [19]), as also assumed by other concrete constitutive models

(e.g. [14]). Thus, the proper framework for the CDP model is that of *elastoplastic coupling* ([9],[12]).

## 2.2 Strain-induced anisotropy of the CDP model

In the undamaged state, concrete is assumed to be isotropic and linear elastic, and the corresponding elastic stiffness tensor is given by Eq. (3). After inelastic phenomena (linked to plastic strains and stiffness degradation) have occurred, either in tension or in compression, the material response is ruled by the following stress-strain law

$$\sigma_{ij} = [1 - r(\bar{\sigma}_{ij})D_t](1 - D_c)E_{ijkl}^0 \varepsilon_{kl}^e. \quad (8)$$

Moreover, the spectral representations of elastic strain and effective stress tensors:

$$\varepsilon_{ij}^e = \sum_{K=1}^3 \varepsilon_K^e \hat{e}_i^K \hat{e}_j^K; \quad (9a)$$

$$\bar{\sigma}_{ij} = \sum_{K=1}^3 \bar{\sigma}_K \hat{e}_i^K \hat{e}_j^K, \quad \bar{\sigma}_K = \lambda_0 \varepsilon_{ii}^e + 2G_0 \varepsilon_K^e; \quad (9b)$$

show that  $\bar{\sigma}_{ij}$  and  $\varepsilon_{ij}^e$  are coaxial due to the isotropic nature of  $E_{ijkl}^0$ ,  $\hat{e}_i^K$  being the common principal directions. Substitution of Eqs. (9) into Eq. (8) leads to the following spectral decomposition of the nominal stress tensor:

$$\sigma_{ij} = \sum_{K=1}^3 [1 - \hat{r}(\varepsilon_{ij}^e)D_t](1 - D_c)\bar{\sigma}_K \hat{e}_i^K \hat{e}_j^K; \quad (10)$$

where

$$\hat{r}(\varepsilon_{ij}^e) = \begin{cases} 0 & \text{if } \varepsilon_{ij}^e = 0 \\ \frac{\sum_{K=1}^3 (\lambda_0 \varepsilon_{ii}^e + 2G_0 \varepsilon_K^e)}{\sum_{K=1}^3 |\lambda_0 \varepsilon_{ii}^e + 2G_0 \varepsilon_K^e|} & \text{otherwise;} \end{cases} \quad (11)$$

is weight function  $r(\bar{\sigma}_{ij})$  expressed in terms of the principal values of the elastic strain tensor.

Previous Eq. (10) states that the principal values of nominal stress  $\sigma_{ij}$  are piecewise-smooth invariant functions of the principal values of  $\varepsilon_{ij}^e$ . Then, according to a known theorem for elastic (or Cauchy elastic) materials [15], the nominal stress is an isotropic function of the elastic strain. Hence,  $\sigma_{ij}$  is always coaxial to  $\varepsilon_{ij}^e$ , as much as  $\bar{\sigma}_{ij}$ . No strain-induced anisotropy should then be observed, in

contrast with the rotating crack model [21]. Therefore, stiffness degradation cannot induce any anisotropy in the response of the CDP model. In other words, when plastic strains are negligible with respect to total strains, such that  $\varepsilon_{ij} \approx \varepsilon_{ij}^e$ , the material behaviour is isotropic.

The only source of induced anisotropy of the CDP model at the local level is linked to the development of plastic strains, which is ruled by the effective stress path and by dilatancy. These theoretical statements are confirmed by numerical simulations of Willam's test illustrated in ensuing Section 3. However, the local isotropy of the CDP secant stiffness should not be viewed as a limitation, in that global anisotropy experienced at the structural level as a consequence of localized cracking may still locally be represented by an isotropic model: a crack would then be interpreted as the geometrical locus of isotropically damaged points/elements [16].

### 3 CONSTITUTIVE RESPONSE OF THE CDP MODEL TO WILLAM'S TEST

In this section, the concrete tensile-dominated response with prescribed rotating principal axes of strain, as predicted by the CDP model, is numerically evaluated with the purpose of assessing its performance in terms of plastic strain-induced anisotropy. Assuming a homogeneous strain field, the constitutive response within the concrete specimen is interpreted as a numerical experiment at the material point level. Thus, reference is made to a single plane four-node finite element, with a single integration point, under plane stress conditions (no confinement in the out-of-plane direction). The element (or material point) is subjected to a nonproportional, strain driven loading with rotating principal directions of strains, as per the so-called Willam's test, originally devised by Willam et al. [21], to compare fixed vs. rotating crack models with plastic softening models. This numerical test has become widely used to verify and compare constitutive models for cracking and damage [7].

Initially, the continuum is subjected to tensile straining in the  $x_1$ -direction accompa-

nied by transverse Poisson's contraction in the  $x_2$ -direction, i.e.  $\dot{\varepsilon}_{11}:\dot{\varepsilon}_{22}:2\dot{\varepsilon}_{12} = 1:-\nu_0:0$ . Immediately after cracking initiation, a switch is made to combined biaxial extension and shear deformation, according to scheduled ratios  $\dot{\varepsilon}_{11}:\dot{\varepsilon}_{22}:2\dot{\varepsilon}_{12} = 0.5:0.75:1$ , as further suggested in [20] and later adopted, e.g. in [6], [14],[16],[22]. Such imposed strains force the continuous rotation of the principal strain directions after crack nucleation, as later shown in Figure 3c. The strain rotation rate is faster at the beginning and progressively slower later on, with a final asymptotic rotation value of about  $52.02^\circ$ .

In the numerical simulations, performed within ABAQUS [1], coordinate axes  $x_1$  and  $x_2$  are referred to  $x$  and  $y$ , respectively. The constitutive analysis requires pertinent small load increments, to minimize computational errors. The backward Euler scheme is adopted to solve for the stress response under imposed strain increments.

#### 3.1 Validation of the implemented Willam's test

With the purposes of assessing the consistency of the present constitutive implementation of Willam's test, comparison is first made to the results recently reported by Wosatko et al. [22], who studied, among other constitutive models, the performance of the CDP model for different values of CDP dilatancy angle  $\psi'_d = \tan^{-1} \alpha'_d$ , mainly by therein neglecting the effects of damage. Thereby, the concrete response also incorporating the effects of damage function  $D_t(\varepsilon_t^i)$  was reported for a single value of dilatancy angle ( $\psi'_d = 25^\circ$ ). Herein, such latter case and the pure elastoplastic response assuming a rather high value of dilatancy angle ( $\psi'_d = 55^\circ$ ) have been considered for the validation purposes.

In Figure 1, the resulting in-plane cartesian stress components,  $\sigma_{xx}$ ,  $\sigma_{yy}$ ,  $\sigma_{xy}$ , and the resulting principal stresses,  $\sigma_I$ ,  $\sigma_{II}$ , are plotted against the prescribed strain along the  $x$ -axis,  $\varepsilon_{xx}$ , which is taken as a reference driving variable in all subsequent plots. The present outcomes appear in good agreement with those

reported in [22], for all the stress components, despite the limited accuracy that can be achieved by graphically tracing their plots (both input data and relevant results). The values of  $\sigma_{xx}$  and  $\sigma_I$  attain at most a value equal to concrete uniaxial tensile strength  $f_{t0} = 3.0$  MPa, at the end of the first phase of Willam's test. Then, stresses  $\sigma_{xx}$  and  $\sigma_I$  decrease by softening, in the second phase, but more rapidly than for the uniaxial curve, as an effect of the mixed stress-strain conditions. Only when damage is active (Figure 1a), all stress components approach zero at the final stage as  $D_t \rightarrow 1$ . In fact, the complete depletion of material integrity driven by damage also releases any residual stress associated to plastic strains. This in turn destroys any form of anisotropy induced by cumulated plastic strains, so that the material behavior returns to isotropy, in the limit of very large strains.

In the absence of damage and for a rather high value of dilatancy angle of the CDP model (Figure 1b), residual stresses arise at the end of the second phase of the test, as a result of non-zero effective stresses induced by choked in-plane dilatant plastic expansion predicted by Eq. (5). This plastic flow clearly reflects the pure plastic nature of the modelled concrete behaviour. Thus, minor principal stress  $\sigma_{II}$  becomes negative, as  $\sigma_I$  decreases to maintain an almost constant gap with  $\sigma_{II}$ , equal to twice the shear stress, as determined by the residual friction angle.

By zooming in Figure 1b around  $\varepsilon_{xx} = \varepsilon_{t0}$ , where  $\varepsilon_{t0} = f_{t0}/E_0 \approx 0.0001$  is the elastic strain at tensile stress peak, it is shown that both stresses  $\sigma_{yy}$  and  $\sigma_{II}$  become negative at the very beginning of the second phase of Willam's test, just before starting growing towards positive values as vertical strain  $\varepsilon_{yy}$  increases, because of dilatancy. This feature of the model response was likely not apparent in [22], and is herein observed by a fine integration step within the constitutive driver.

### 3.2 Parametric analyses

To verify and extend the above-mentioned considerations and to accurately investigate the effect of damage and dilatancy on the CDP

model response during Willam's test, a parametric study can be carried out, at this stage, whose input and results are discussed in following Sections 3.2.1 and 3.2.2. The investigation is focused on the possibilities to capture rotations of the principal directions of stress beyond cracking. The assumed mechanical properties of concrete needed by the CDP model during the present parametric analysis are first described next.

#### 3.2.1 Definition and parametrization of the constitutive law

The constitutive CDP model described in Section 2.1 allows to formulate a variety of material behaviors by suitably varying the post-peak strength and damage functions ( $f_t, f_c, D_t, D_c$ ) and the underlying characteristic parameters ( $E_0, \nu_0, \alpha, \gamma, \alpha'_d$ ).

For tension and tension-shear dominated problems, the concrete nonlinear response in compression is not mobilized. Thus, to minimize complexity, an adequate form of the CDP model can be achieved by defining functions  $f_t(\varepsilon_t^i)$  and  $D_t(\varepsilon_t^i)$  governing the concrete inelastic response under tensile dominated stress states. The exponential softening functional form [4] is herein adopted, for describing the evolution of  $f_t(\varepsilon_t^i)$ , i.e.:

$$f_t(\varepsilon_t^i) = f_{t0} \exp\left(-\frac{f_{t0}}{g_t^f} \varepsilon_t^i\right); \quad (12)$$

showing that exponential softening is completely specified by tensile strength  $f_{t0}$  of the undamaged concrete and specific fracture energy in tension  $g_t^f$ . The integration over inelastic strain  $\varepsilon_t^i$  of Eq. (12), with  $\varepsilon_t^i$  ranging from 0 to infinity, is exactly equal to  $g_t^f$ , which clearly gives its meaning. The fact that  $g_t^f$  is one of the given material parameters, is also rather convenient for possibly implementing fracture-energy regularization procedures at the finite element level and structural scale (an aspect herein not inquired).

In the CDP model, total inelastic strains are the sum of plastic strains and irreversible increments of elastic strains prompted by damage. Then, a simple model for plastic

microcracking is obtained by further assuming that the plastic strain under uniaxial tension is a constant fraction of the total inelastic strain, say,  $\varepsilon_I^p = \alpha_p \varepsilon_I^i$ , where  $0 < \alpha_p \leq 1$  is taken as a material constant [17].

Accordingly, damage evolution function  $D_t(\varepsilon_I^i)$  follows from plastic to inelastic strain ratio  $\alpha_p$  and from the expression of  $f_t(\varepsilon_I^i)$  given in Eq. (12):

$$\begin{aligned} \varepsilon_I^i &= \varepsilon_I^p + \varepsilon_I^{ed} = \alpha_p \varepsilon_I^i + \frac{D_t(\varepsilon_I^i)}{1 - D_t(\varepsilon_I^i)} \frac{f_t(\varepsilon_I^i)}{E_0}; \\ \rightarrow D_t(\varepsilon_I^i) &= \left[ 1 + \frac{f_t(\varepsilon_I^i)}{(1 - \alpha_p)E_0 \varepsilon_I^i} \right]^{-1}. \end{aligned} \quad (13)$$

Both functions  $f_t(\varepsilon_I^i)$  and  $D_t(\varepsilon_I^i)$  are depicted in Figure 2, considering an undamaged Young's modulus of  $E_0 = 21500 f_{t0}$ , as provided by the CEB-FIP Model Code (1990) formula [13], for a typical ratio of compressive strength/tensile strength ( $f_{c0}/f_{t0}$ ) equal to 10. The initial compressive strength  $f_{c0} = 10f_{t0}$  is kept fixed during the entire analysis due to its negligible effect during Willam's test. Poisson's ratio  $\nu_0$  is assumed equal to 0.2.

Damage evolution function  $D_t(\varepsilon_I^i)$  is plotted in Figure 2b for two distinct values of plastic to inelastic strain ratio  $\alpha_p$ . One is quite small ( $\alpha_p = 0.01$ ), but greater than zero (inelasticity of the CDP model is led by plastic strains, which cannot be suppressed), indicating a nearly isotropic damage model; the other is placed right in the middle of the range of  $\alpha_p$  ( $\alpha_p = 0.5$ ), pointing out to a coupled model in which both stiffness degradation and plastic flow equally contribute to the total inelastic strains ( $\alpha_p = 0.5$ ). Upper limit  $\alpha_p = 1$ , denoting a CDP model degenerating to a pure softening elastoplastic material formulation (with no damage), already addressed in [22], is not herein reconsidered.

The remaining parameters of the CDP model are the eccentricity of the plastic potential ( $e = 0.1$ ) and the shape parameters of the yield function, namely  $\alpha = 0.121$ , corresponding to a ratio of the biaxial to the uniaxial compressive strength of 1.16, and  $\gamma = 3$ , which is obtained by setting the ratio between the radii of the

tensile and compressive meridians on the deviatoric plane equal to the standard value of  $2/3$ .

### 3.2.2 Results

A graphical representation of the normalized constitutive response of the CDP model for all the in-plane stress components, both cartesian and principal, gained from the numerical simulation of Willam's test is provided in Figure 3 and in Figure 4, for the two selected values of plastic to inelastic strain ratio  $\alpha_p$  and the three assumed values of CDP dilatancy angle  $\psi'_d$ . The considered range of CDP dilatancy angle, going from  $15^\circ$  to  $55^\circ$ , shall encompass the almost entire range of expected experimental values for concrete.

For  $\alpha_p = 0.01$ , the stress response is consistently unaffected by the dilatancy angle (Figure 3a-b), since plastic strains are kept to a minimum and the overall inelastic deformation is attributed to isotropic stiffness degradation. As expected from the underlying isotropy argument, the principal stress directions coincide with the prescribed principal strain directions, i.e. stress-strain axes co-rotate, independently of  $\psi'_d$  (Figure 3c). Only at rather large strains (e.g.  $\varepsilon_{xx} > 6\varepsilon_{t0} = 6f_{t0}/E_0$ ) some slight deviation from coaxiality can be appreciated, due to the development of small plastic strains. Hence, numerical outcomes corroborate the theoretical statements of preceding Section 2.2, in that no anisotropy is manifested by the constitutive model, whenever plastic strains remain marginal.

When non-negligible plastic strains are accounted for ( $\alpha_p = 0.5$ ), during the second phase of Willam's test both  $\sigma_{yy}$  and  $\sigma_{xy}$  stress components increase with respect to those predicted by the "pure" damage model ( $\alpha_p = 0.01$ ), because of the damped stiffness degradation, attested by Figure 2b. The increase of  $\sigma_{yy}$  is such that, at some point, it overcomes  $\sigma_{xx}$  (Figure 4a-b), a feature also revealed by other constitutive models tried along Willam's test ([6],[14]).

As concrete dilatancy rises, for fixed total strains, plastic strains growth, to the detriment of elastic strains, thus reducing  $\sigma_{yy}$  and  $\sigma_{II}$ ; on

the other hand, shear stress component  $\sigma_{xy}$  benefits from such an additional compressive strength promoted by dilatancy.

The plot of the angle of rotation of principal stress directions (Figure 4c) substantially differs from that of the “pure” isotropic damage one (Figure 3c), revealing that plastic strain-induced anisotropy accelerates the rotation of the principal stresses, almost independently from the value of the CDP dilatancy angle. The positive values of plastic strains (opening cracks), as predicted by the normal to the DP plastic potential, explain why stress increments over-rotate with respect to strain increments. All rotations trends are bounded by asymptotic strain angle  $52.02^\circ$  and never exceed that value, as instead indicated by different anisotropic damage modes ([5],[6],[16]).

From Figure 4c, it is apparent that the rotation rate of principal stress components is drastically reduced around  $\varepsilon_{xx} = 3\varepsilon_{t0}$ , and gradually converges towards the final asymptotic value of the strain rotation. In fact, as an important remark, as the prescribed strains increase, damage withdraws plastic strain-induced-anisotropy, so that the material behaviour tends to become again fully isotropic, in the limit of very large strains.

#### 4 CONCLUSIONS

In the present paper, the quite popular Lee-Fenves’ CDP constitutive model (available within the ABAQUS platform) has been scrutinized to provide useful insights on its current abilities and limitations in the modelling of the nonlinear behaviour of quasi-brittle materials, such as concrete, under rather complex loading paths. In particular, this investigation has been set with the goal of investigating the conditions under which an anisotropic behaviour may be predicted under multiaxial stress states. The following main points have been targeted and recorded:

- The conditions under which an anisotropic behaviour may be predicted by the CDP model under multiaxial stress states have been investigated through an analysis of the constitutive equations of the model, highlighting that the only source of induced

anisotropy at the local level arises from the development of plastic strains, which also drive all the inelastic phenomena reproduced by the model. Plastic strains are ruled by the effective stress path and by dilatancy.

- The formulation statements have been confirmed by numerical simulations of the CDP model response to a peculiar non-radial loading path (Willam’s test). The analyses have been implemented and performed at a constitutive-driver level within ABAQUS.
- A consistent validation of the present implementation has been achieved, based on results of a couple of Willam’s tests recently reported in [22], for the comparison of different models. The latter have been adopted as a benchmark reference, for the numerical solution, with arising rather close matchings and commented relevant highlighted numerical and physical findings, which are per se interesting, for the interpretation of the CDP model capabilities.
- A parametrization of prescribed tensile damage evolution function  $D_t(\varepsilon_t^i)$  in terms of corresponding post-peak strength function  $f_t(\varepsilon_t^i)$  has been achieved, through a single suitable scalar parameter, i.e. plastic to inelastic strain ratio  $\alpha_p$ , along the line of Ortiz’s proposal [17].
- Non-dimensional curves of both cartesian and principal stress components have been presented, for two values of  $\alpha_p$  and three values of CDP dilatancy angle  $\psi'_d$ , showing several important and characteristic features of the CDP constitutive response. Namely:
  - the results of the Willam’s test can result rather different, even if a source identical behaviour in the uniaxial tension softening curve is adopted, by varying  $\alpha_p$ ; dilatancy angle  $\psi'_d$ , instead, displays a minor effect on the stress response, except for the case in which plasticity is overriding stiffness degradation (slight or no damage);
  - when plastic strains are overall negligible (worked case of  $\alpha_p = 0.01$ ), though still driving the inelastic response, stress-strain axes co-rotate, independently

of  $\psi'_d$ ; as opposed, when plastic strains are accounted for (worked case of  $\alpha_p = 0.5$ ), plastic strain-induced anisotropy appears, so that stress increments over-rotate with respect to strain increments;

- in the presence of stiffness degradation, damage further withdraws plastic strain-induced-anisotropy at quite large strains, over the softening range, so that the material behavior returns fully isotropic, in the limit of very large strains.

Further investigations on features and outcomes of the CDP model, for both theoretical and numerical scenarios, at the constitutive scale, and possibly at the structural scale, may elsewhere be reported, where more room shall become available.

## REFERENCES

- [1] ABAQUS (2024), Version 2024, Dassault Systèmes Simulia Corp., USA.
- [2] Bažant Z.P. (1980), Work inequalities for plastic fracturing materials, *Int. J. Solids Struct.*, **16(10)**, 873–901.
- [3] Bažant Z.P. and Oh B.H. (1983), Crack band theory for fracture of concrete, *Matér. Constr.*, **16(93)**, 155–177.
- [4] Bažant Z.P., Planas J. (1998), *Fracture and Size Effect in Concrete and Other Quasibrittle Materials*, CRC Press, London, UK.
- [5] Carol I., Rizzi E., Willam K.J. (2001), On the formulation of anisotropic elastics degradation. I. Theory based on a pseudo-logarithmic damage tensor rate, *Int. J. Solids Struct.*, **38(4)**, 491–518.
- [6] Carol I., Rizzi E., Willam K.J. (2001), On the formulation of anisotropic elastics degradation. II. Generalized pseudo-Rankine model for tensile damage, *Int. J. Solids Struct.*, **38(4)**, 519–546.
- [7] Carol I., Rizzi E., Willam K.J. (2008), Discussion on the paper: application of some anisotropic damage model to the prediction of failure of some complex industrial concrete structure, *Int. J. Solids Struct.*, **45(16)**, 4600–4602 [Badel P., Godard V., Leblond J.-B. (2007), *Int. J. Solids Struct.*, **44(18-19)**, 5848–5874].
- [8] Grassl P., Jirásek M. (2006), Damage-plastic model for concrete failure, *Int. J. Solids Struct.*, **43(22-23)**, 7166–7196.
- [9] Hueckel T., Maier G. (1977), Incremental boundary value problems in the presence of coupling of elastic and plastic deformations: a rock mechanics oriented theory, *Int. J. Solids Struct.*, **13(1)**, 1–15.
- [10] Lee J., Fenves G.L. (1998), Plastic-damage model for cyclic loading of concrete structures, *J. Eng. Mech. (ASCE)*, **124(8)**, 892–900.
- [11] Lubliner J., Oliver J., Oller S., Onate E. (1989), A plastic-damage model for concrete, *Int. J. Solids Struct.*, **25(3)**, 299–326.
- [12] Maier G., Hueckel T. (1979), Nonassociated and coupled flow-rules of elastoplasticity for rock-like materials, *Int. J. Rock Mech. Min. Sci.*, **16(2)**, 77–92.
- [13] Mehta P.K., Monteiro P.J.M. (2006), *Concrete: Microstructure, Properties, and Materials*, 3rd Ed., McGraw-Hill, New York, USA.
- [14] Meschke G., Macht J., Lackner R. (1998), A damage-plasticity model for concrete accounting for fracture-induced anisotropy. In: Mang H., Bićanić N., de Borst R. (eds.), *Computational Modelling of Concrete Structures*, Balkema, Badgastein, Austria; pp. 3–12.
- [15] Ogden R.W. (1997), *Non-linear Elastic Deformations*, Dover Publications Inc., Mineola, New York (USA).
- [16] Oliver J., Cervera M., Oller S., Lubliner J. (1990), Isotropic damage models and smeared crack analysis of concrete. In: Bićanić N., Mang H. (eds.), *Computer-Aided Analysis and Design of Concrete Structures*, vol. 2, Pineridge, Zell-am-See, Austria; pp. 945–957.
- [17] Ortiz M. (1985), A constitutive theory for the inelastic behavior of concrete, *Mech. Mater.*, **4(1)**, 67–93.
- [18] Pramono E., Willam K. (1989), Fracture

energy-based plasticity formulation of plain concrete, *J. Eng. Mech. (ASCE)*, **115(6)**, 1183–1203.

- [19] Rizzi E., Maier G., Willam, K. (1996), On failure indicators in multi-dissipative materials, *Int. J. Solids Struct.*, **33(20-22)**, 3187–3214.
- [20] Rots J.G. (1988), *Computational Modelling of Concrete Fracture*, Ph.D. Thesis, Delft University of Technology, Delft, The Netherlands, 141 pages.
- [21] Willam K., Pramono E., Sture S. (1987), Fundamental issues of smeared crack models, In: Shah S.P. and Swartz S.E.

(eds), *Proceedings of SEM/RILEM International Conference of Fracture and Rocks*, Springer, Berlin, Germany, 142–157, Houston, Texas (USA), June 17–19.

- [22] Wosatko A., Szczecina M., Winnicki A. (2020), Selected concrete models studied using Willam's test, *Mater.*, **13(21)**, 4756–4779.
- [23] Xotta G., Beizae S., Willam K.J. (2016), Bifurcation investigations of coupled damage-plasticity models for concrete materials, *Comput. Methods Appl. Mech. Eng.*, **298**, 428–452.

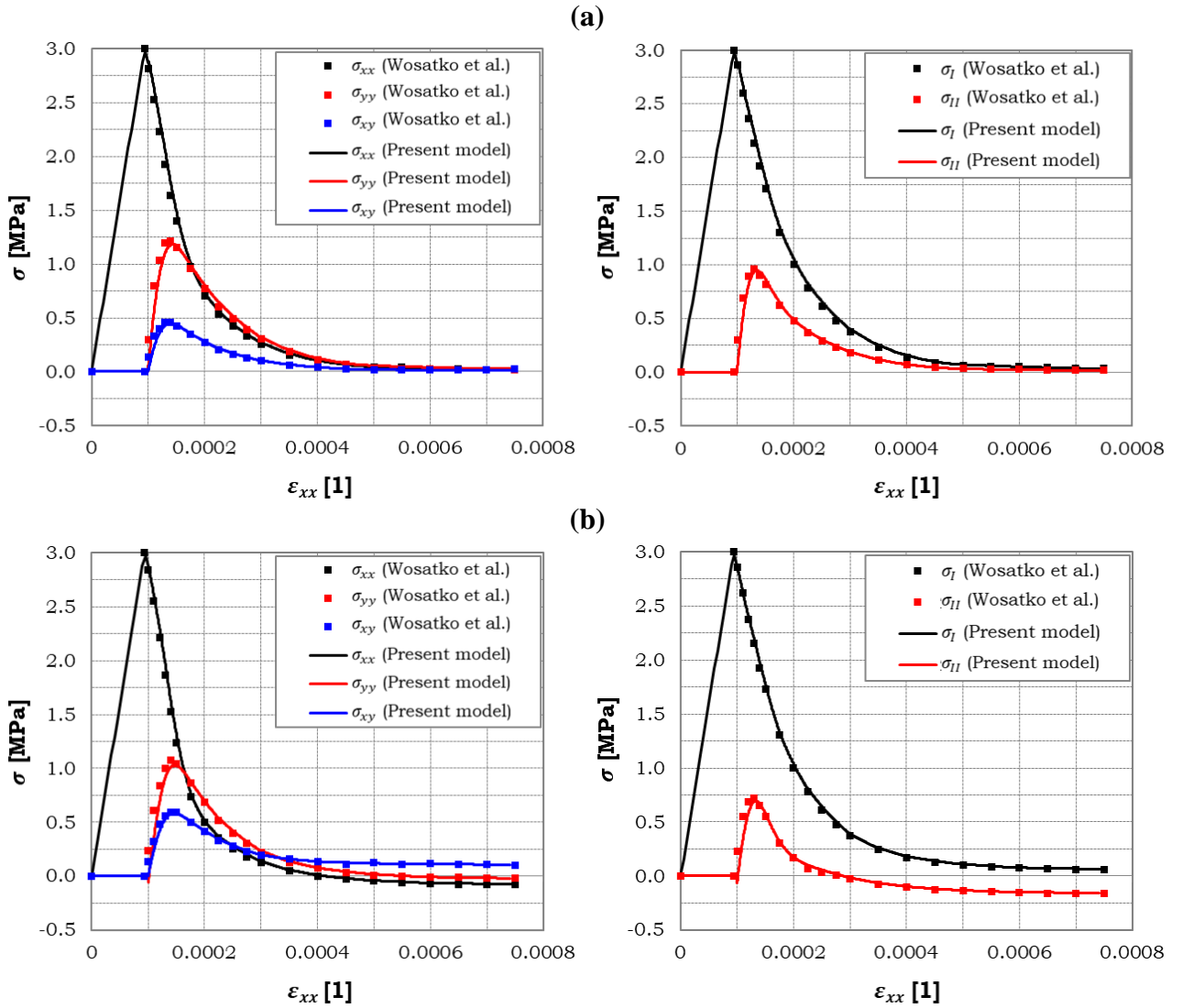


**Figure 1:** Comparison of stress components obtained from Willam's test with those reported by Wosatko et al. [22]: (a) elastoplasticity coupled with damage ( $\psi'_d = 25^\circ$ ,  $D_t(\epsilon_i^i) \neq 0$ ) and (b) pure elastoplastic behaviour ( $\psi'_d = 55^\circ$ ,  $D_t(\epsilon_i^i) = 0$ ); first column: cartesian stress components; second column: principal stress components.

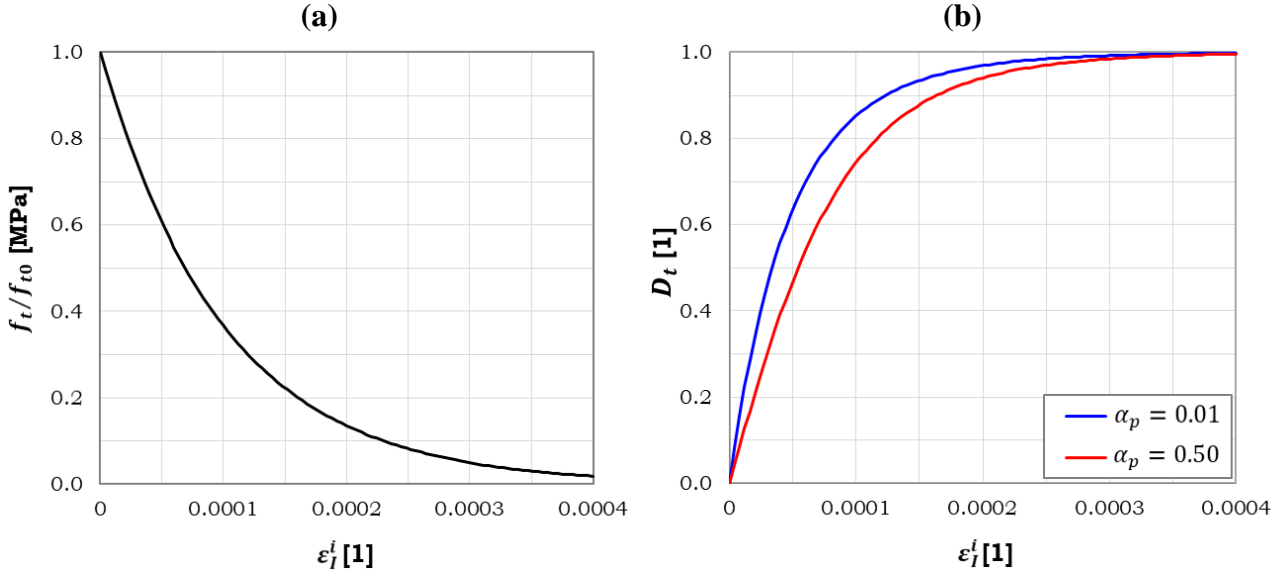


**Figure 2:** Evolution of adopted concrete (a) tensile strength and (b) tensile damage as a function of major principal inelastic strain

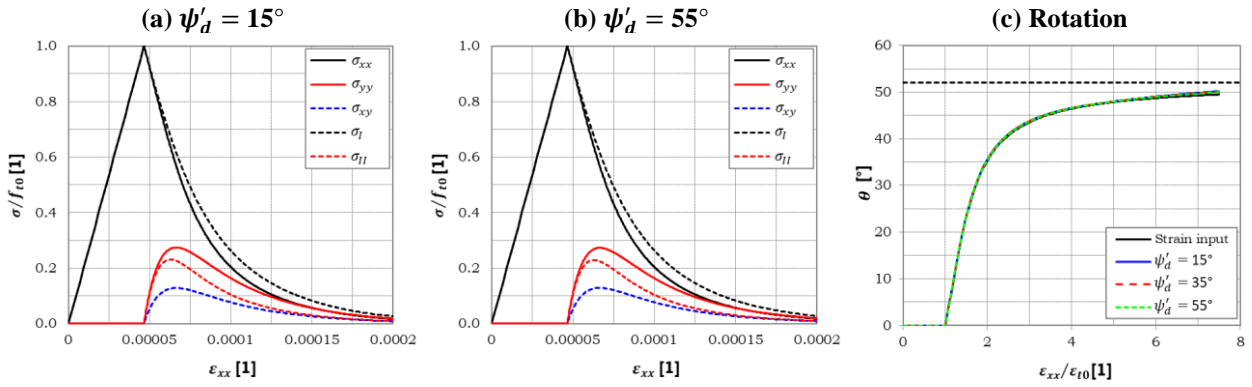


**Figure 3:** Results of CDP model subjected to Willam's test for  $\alpha_p = 0.01$ : stress components calculated for (a)  $\psi'_d = 15^\circ$  and (b)  $\psi'_d = 55^\circ$ ; (c) imposed rotation of major principal strain axis and rotation of major principal stress axes for different values of  $\psi'_d$

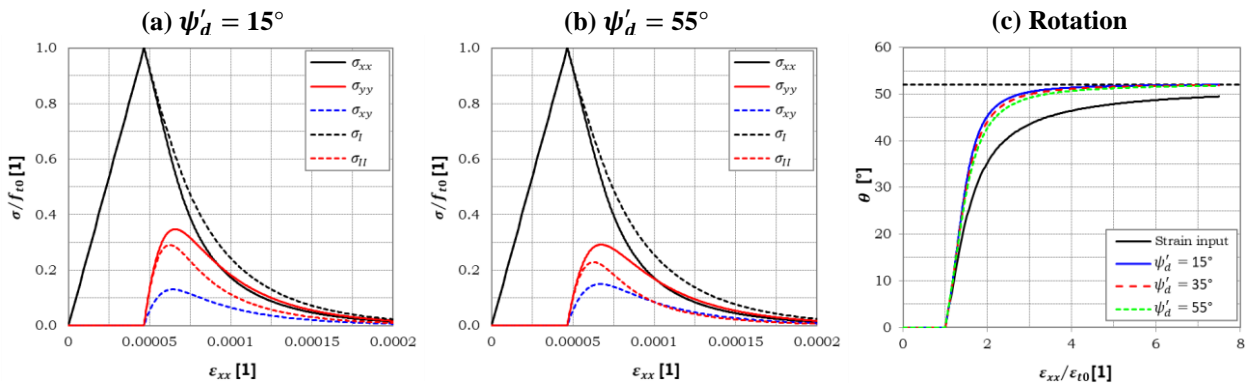


**Figure 4:** Results of CDP model subjected to Willam's test for  $\alpha_p = 0.5$ : stress components calculated for (a)  $\psi'_d = 15^\circ$  and (b)  $\psi'_d = 55^\circ$ ; (c) imposed rotation of major principal strain axis and rotation of major principal stress axes for different values of  $\psi'_d$